Elastic strains and coherency stresses in Mo/Ni multilayers

J. A. Bain and L. J. Chyung
Department of Materials Science and Engineering, Stanford University, Stanford, California 94305-2205

S. Brennan
Stanford Synchrotron Radiation Laboratory, Stanford, California 94309

B. M. Clemens
Department of Materials Science and Engineering, Stanford University, Stanford, California 94305-2205
(Received 15 January 1991)

The observed expansion in the out-of-plane lattice parameter in metal multilayers can be produced by elastic strains, bulk relaxation, or interface dilatation. Each can produce the observed out-of-plane result but will differ in their in-plane lattice-parameter behavior. We perform a complete strain determination in Mo/Ni multilayers, using grazing-incidence and asymmetric x-ray diffraction as well as substrate-curvature-stress measurements, and determine that elastic strains dominate. Assuming Nishiyama-Wasserman epitaxial orientation, we were able to calculate the complete stress state in both materials. The stresses, which arise from substrate interaction and coherency between the bcc Mo and fcc Ni layers, increase as the bilayer period is decreased. We find remarkable agreement between the substrate-interaction stresses calculated from x-ray strain measurements and those measured using wafer-curvature techniques; this shows that interface contraction stresses are not significant. We found no evidence for interface dilatation strains. Furthermore, the small changes that are observed in the unstrained lattice parameters can be ascribed to alloying rather than bulk relaxation.

I. INTRODUCTION

Recent work on multilayer films has demonstrated an expansion of the lattice-plane spacing in the growth direction which varies with bilayer period.[1–3] Over some bilayer period range, the out-of-plane lattice spacing is observed to increase linearly with the reciprocal of the bilayer period, so that the effect is proportional to interface density. This variation may be attributed to elastic strain arising from changes in residual stresses, bulk relaxation due to electronic transfer effects,[4] or interface dilatation[2]. Although each can produce the observed behavior in the out-of-plane lattice spacing, we find, through a complete determination of the stress state of the constituents, that elastic strains due to stresses dominate. In particular, we find coherency stresses and a compressive substrate interaction stress that increase as the bilayer period decreases.

II. CLASSIFICATION OF STRAINS IN MULTILAYERS

To see how systematic variations in elastic strain due to residual stress can result in the observed behavior, we first classify the stresses in multilayers according to their sources. We consider the possible sources of stresses on a given layer to be the substrate, the bounding constituents, and the interfaces (as distinct entities). X-ray diffraction measures a final state in which the total stress in each layer is a superposition of these three types. Any combination of these which produces a compressive stress which decreases with increasing bilayer period will produce the observed behavior in the x-ray-diffraction spectra. This results from an out-of-plane Poisson expansion which scales with the in-plane stress and produces the observed shift in the lattice parameter with bilayer period.

Before we discuss each stress source in more detail, we first make some general comments concerning the thickness dependence of stress in an individual layer. Strain in a thin film or layer can be accommodated by either plastic deformation or elastic strain (with its concomitant stress). In the case of coherency strains, Matthews has shown that, once a critical thickness is exceeded, the energy balance between elastic strain and deformation defects (e.g., misfit dislocations at the interface) will result in stresses which decrease with increasing layer thickness.[5] Nix has shown that this effect is independent of the source of the strain, and can be represented as a yield stress which decreases as the film thickness increases.[6] In most thin-film mechanical problems, the growth parameters and material choices set an imposed constant strain. In light of this, it is useful to think of a thickness-dependent yield *strain* , which is the portion of the imposed strain which can be accommodated elastically at any thickness. When a film reaches its critical thickness, defects begin to form, and thereafter, the elastic strain in the film is always at its yield value, which falls as the film thickens. It immediately follows that all films above their critical thickness will be supporting their yield stress which will also decrease with film thickness.

Substrate-interaction stresses are usually caused by morphological rearrangement in the film. The volume change associated with alloying, defect annihilation, grain growth, island agglomeration, and differential thermal expansion will be opposed by the substrate. A

 ©1991 The American Physical Society

compressive substrate-interaction stress means that the substrate compresses the film in the plane of the film. An out-of-plane Poisson expansion of the film will accompany the in-plane contraction of the film. The top substrate surface will be convex as the substrate bends in response to the opposing force in the film. In sputtered films, compressive stresses are commonly observed at low sputtering pressures.[7]

Alternatively, it has been proposed that compressive substrate-interaction stresses can arise during growth from the action of surface stresses. These stresses result from the free-energy decrease associated with a reduction in surface area[8–10] and will cause an in-plane compressive stress during the initial stages of growth. As the film thickens, however, the surface plays an increasingly smaller role; subsequent growth will either introduce plastic deformation or require a compressive substrate interaction to maintain the strain level set by the first monolayer under the influence of the surface stress.

We observe, as have others,[11] a compressive substrate-interaction stress which increases with decreasing bilayer period in multilayer films. This can produce the observed lattice-plane expansion behavior. At this point, we choose not to speculate on the source of this stress, but we point out that its behavior with layer thickness can be understood in terms of the thickness-dependent yield strain discussed above.

In multilayers, the substrate-interaction stress acts equally on each layer in the entire film, but there can also be stresses between the individual constituent layers. These coherency stresses arise from the attempt to minimize interface energy by matching the lattices of the two constituents. As discussed above, if the lattice misfit results in the formation of misfit dislocations, the stress will decrease as the layer thickness increases. The observed change of the atomic-plane spacing in the growth direction will occur if the material in tension is elastically stiffer than the material in compression.

Coherency stresses may be distinguished from substrate-interaction stresses by their dependence on crystallographic direction. This difference stems from the difference in the way the local stresses of each type are correlated with crystallographic direction. Local substrate-interaction stresses will vary from crystallite to crystallite, but will have no correlation with crystallographic direction. The measured substrate-interaction stress, which is assumed to be equal-biaxial, will be the average of the stresses in the individual crystallites. Since the local substrate-interaction stresses within each crystal will have no directional relationship to the crystallographic axes of the crystallite, the average substrate-interaction stress will be independent of crystallographic direction.

In contrast, we expect the direction of the principal coherency stresses to correlate with the crystallographic axes, since these stresses arise from the attempts of the two constituent layers to match their lattice parameters and symmetry. In the case where the two mating planes have different symmetry, such as in the present case where we consider Mo bcc (110) planes mating with Ni fcc (111) planes, coherency stresses may vary with crystallographic orientation. For example, if the coherency stresses "conspire" to match the spacing *between* rows of atoms along a particular direction in the two constituents, the largest value of stress will be expected to lie perpendicular to the atom rows. Therefore, coherency stresses will not be equal-biaxial, and will result in in-plane lattice parameters which depend on the crystallographic direction in which they are measured.

In addition to substrate-interaction stresses and coherency stresses, interfacial contraction stresses have been postulated to play a role in multilayers. These stresses are postulated to come from interfacial contraction forces analogous to surface tensions discussed above. Cammarata and Sieradzki have suggested that in a free-standing multilayer film, interfacial contraction forces will compress the constituents to the point where elastic restoring forces in the layers balance the interfacial surface tension. As the interface density is increased (bilayer period is decreased), this in-plane contraction will increase, and the required variation with bilayer period results.[12] In a multilayer film on a substrate, the substrate will hinder this contraction and will bear at least part of the interface tension load.[13] The top of the substrate would be concave, as though curved by a film under a tensile substrate-interaction stress. In actuality, it would be the interfaces in tension while the multilayer would experience a slight compressive stress due to the curvature of the substrate. Thus, if interfacial contraction stresses are significant, the stress in the constituent layers (which we calculate from changes in lattice parameters of the constituents) will be less tensile than the stress observed to be bending the substrate.

Although we find that elastic strains can account for the observed lattice-plane expansion in the growth direction, it is instructive to examine some of the other mechanisms which have been proposed to account for this phenomenon. If interfacial disorder or the presence of interfacial defects causes the atomic planes at the interface to have a greater separation than the constituents, an increase in the number of interfaces will produce an increase in the observed lattice-plane spacing in the growth direction.[2] In this case, interfacial dilatation results from interface morphology. A second proposed source of interface dilatation is relaxation, where the lattice spacings at the interface differ from the bulk due to electronic effects. The resulting displacements are not due to stresses, and have been observed in computer models.[14] Each of these mechanisms has the characteristic of an anomalous interface lattice spacing which can account for the observed behavior in the out-of-plane lattice spacing. However, unlike the elastic strains, neither is expected to have an effect on the in-plane lattice spacings. It has also been suggested that electron-transfer effects can result in a bulk expansion which will produce the observed out-of-plane lattice spacing behavior.[4] Presumably this occurs when the expansion of the constituent receiving electrons is greater than the contraction experienced by the electron-donating constituent.

To summarize, stresses which give rise to elastic strains in multilayers can be classified as coherency stresses, interfacial-contraction stresses, or substrate-interaction

stresses. Each can result in the observed out-of-plane lattice expansion, but each has characteristic behavior which can be distinguished by a complete determination of the strain state of the layers in a multilayer. Substrate-interaction stresses have no directional relationship to crystallographic direction. Interface-contraction stresses will result in a lack of balance between the force exerted by the substrate on the film and the stresses in the constituent layers. Coherency stresses will be equal and opposite in the two constituents, and will produce lattice parameters which depend on crystallographic direction. Other displacement mechanisms include interface dilatation due to interface morphology or relaxation effects, where the observed out-of-plane expansion is due to an anomalous interfacial lattice-plane spacing. Bulk expansion due to electron transfer can also account for the observed behavior.

A. Stress and strain measurement

Much of the analysis of lattice-plane spacing changes in metal multilayers has been done using symmetric x-ray diffraction, which measures lattice spacing in the growth direction. The average lattice parameter in the growth direction can be obtained from the position of the central peak in the high-angle superlattice satellite region.[1,2] The average measured this way will reflect the effect of changes in the lattice parameters of the constituents as well as the effect of anomalous interface atomic-plane spacings. We can write the average obtained from the central superlattice satellite in symmetric diffraction, $\bar{d}_{\perp}^{S}$, as

$$\bar{d}_{\perp}^{S}=\frac{(N^{a}-1)d_{\perp}^{a}+(N^{b}-1)d_{\perp}^{b}+2d_{\perp}^{\text{int}}}{(N^{a}+N^{b})}, \quad (1)$$

where $N^{a,b}$ is the number of atomic planes of a,b per bilayer, $d_{\perp}^{a,b}$ is the growth-direction atomic-plane spacing of constituent a,b, and $d_{\perp}^{\text{int}}$ is the growth-direction atomic-plane spacing at the interface between the last plane of constituent a and the first plane of constituent b and vice versa. This average is affected by both the bulk and interface effects described above, as can be seen if we define an average "bulk" out-of-plane d spacing as

$$\bar{d}_{\perp}^{B}=\frac{N^{a}d_{\perp}^{a}+N^{b}d_{\perp}^{b}}{N^{a}+N^{b}} \quad (2)$$

and an interface expansion, δ, relative to the arithmetic average of the atomic plane spacings of the constituents:

$$\delta=d_{\perp}^{\text{int}}-\frac{d_{\perp}^{a}+d_{\perp}^{b}}{2}. \quad (3)$$

Changes in the lattice parameter of the constituents will be reflected in $\bar{d}_{\perp}^{B}$, while δ is a measure of the interface expansion relative to the constituent average. We can then write $\bar{d}_{\perp}^{S}$ as

$$\bar{d}_{\perp}^{S}=\frac{\bar{d}_{\perp}^{B}}{1-2\delta/\Lambda}\approx\bar{d}_{\perp}^{B}\left[1+\frac{2\delta}{\Lambda}\right], \quad (4)$$

where Λ, is the bilayer period $\left[\Lambda=\bar{d}_{\perp}^{S}(N^{a}+N^{b})\right]$. Systematic changes in elastic strains or bulk expansion will affect $\bar{d}_{\perp}^{S}$ through their effect on $\bar{d}_{\perp}^{B}$, while an interface dilatation, which results in $\delta>0$, will result in an increase in $\bar{d}_{\perp}^{S}$ which is linear in $1/\Lambda$. Symmetric x-ray-diffraction measurements of $\bar{d}_{\perp}^{S}$ can therefore be used to precisely measure either effect, but not to distinguish between the two. It is also not possible to distinguish between the various sources of elastic strain or bulk expansion with only the measurement of $\bar{d}_{\perp}^{S}$.

However, due to the relatively short lateral coherence of our samples, in-plane and asymmetric d-spacing measurements avoid the convolution of the composition modulation and yield the lattice parameters of the individual constituents at various orientations relative to the strain tensor. These lattice-parameter measurements, combined with the elasticity analysis described below, allow us to completely determine the strain and stress in each constituent. Although asymmetric and in-plane measurements have previously been performed on multilayers,[15,16] we believe that this is the first complete determination of constituent stress and strain. We find that coherency stresses and compressive substrate-interaction stresses dominate strain in Mo/Ni multilayers, and that interface-contraction stresses and interface dilatation are not significant. The out-of-plane expansion in $\bar{d}_{\perp}^{S}$ is completely accounted for by elastic coherency and substrate-interaction stresses which increase as the bilayer period is decreased. The coherency stresses are not equal-biaxial, and have the largest component in the direction of largest mismatch.

III. EXPERIMENTAL METHODS

We examined Mo/Ni multilayer films deposited by magnetron sputtering onto [100] Si wafers with amorphous oxide caps of approximately 5000 Å. The details of fabrication are discussed in an earlier work.[2] Bilayer periods vary from 10 to 200 Å, with equal thicknesses of each constituent. The Ni (fcc) develops a strong (111) texture in the growth direction while the Mo (bcc) has a (110) texture in the growth direction. All layers are polycrystalline and exhibit no in-plane orientation relationship with the substrate.

Symmetric reflection x-ray measurements were taken on a Philips XRG 3100 powder diffractometer using Cu $K\alpha$ radiation. Asymmetric plane spacings were measured using a custom-made generalized focusing diffractometer and a rotating anode x-ray source.[17] Grazing-incidence x-ray scattering (GIXS) measurements were made on a Huber four-circle goniometer on beam line 7-2 of the Stanford Synchrotron Radiation Laboratory. A double-crystal monochromator was used at a beam energy of 8210 eV.[18] Peak positions were extracted from the data by fitting to Gaussian peaks with linear or parabolic backgrounds.

The geometry of each type of measurement is discussed in the references, but it is illustrative to consider the orientation of the planes that can be measured with each technique. Figure 1 shows a stereographic projection for the texture in the films along the surface normal. Figure

1(a) shows the projection along the surface normal of bcc constituents and the available reflections in each of the three diffraction modes. Reflections on the perimeter of the projections are available in the GIXS mode at $\omega=90°$, where ω is the angle between the surface normal and a given pole or reflection. The central pole represents the symmetric reflection for perfect texture. Reflections which are available within the constraints of the asymmetric geometry are shown as poles between these two extremes. Figure 1(b) shows the same information for fcc constituents.

Substrate-interaction stresses were measured using an optical-substrate-curvature technique.[19] Substrate curvature was measured before and after stripping the sample film from the substrate to correct for substrate curvature not related to film stresses.

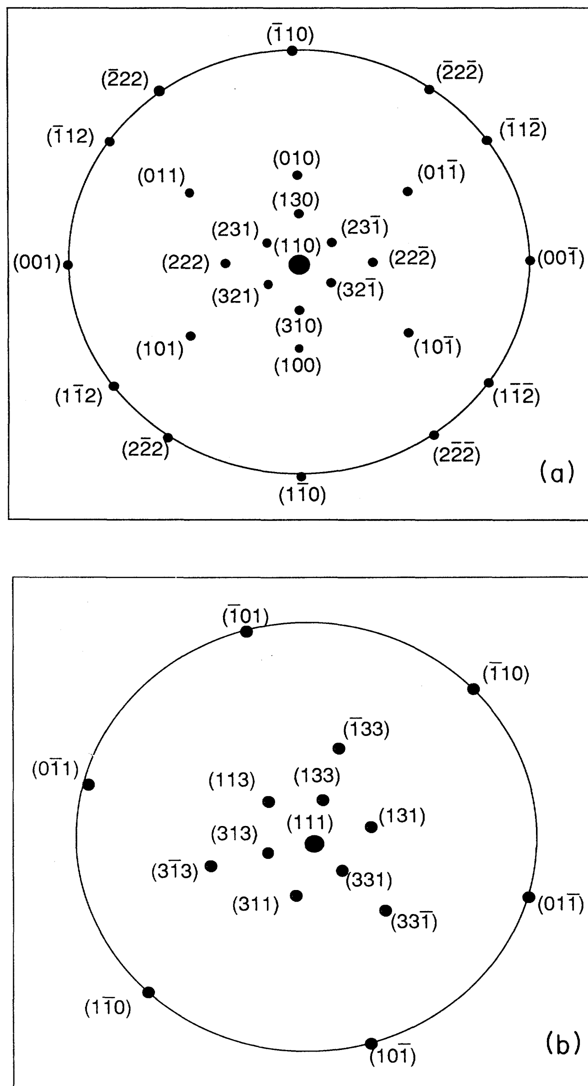

FIG. 1. Stereographic projections of one crystallite in each of the constituents viewed from the sample normals. (a) (110) fiber texture in Mo. (b) (111) fiber texture in Ni.

IV. RESULTS AND DISCUSSION

A. Elasticity analysis

X-ray-diffraction measurements yield the d spacing corresponding to a particular reflection in a given direction, indicated by the indices $\{hkl\}$. The lattice parameter, a, calculated from measured d spacings and their $\{hkl\}$ values, will be affected by the strain resulting from an applied stress. In the case where an anisotropic stress is applied to a single crystal with a known unstrained lattice parameter, the strain, ϵ, along a particular direction can be found from the definition

$$\epsilon=\frac{a-a_0}{a_0}\ , \tag{5}$$

where a_0 is the unstrained lattice parameter. Lattice-parameter measurements in several noncoplanar directions directly yield the strain tensor. In multilayers uncertainty in the unstrained lattice parameter exists due to alloying or relaxation effects, so a_0 for each constituent must be viewed as an unknown parameter. Furthermore, our films are not of single-crystal type, and each measured d spacing is an average of sets of planes which have nonequivalent orientations relative to the strain tensor. These two factors complicate our analysis. However, by utilizing elasticity analysis with an assumption of epitaxial orientation, we are able to extract the stress state of the constituents in our multilayer films. We calculate the lattice parameters that would be observed for an arbitrary stress state, and then fit the measured lattice-parameter values to find the principal stresses and unstrained lattice parameter.

The random in-plane orientation of crystallites in our samples coupled with the multiplicity of reflections results in several sets of planes contributing to any given observed reflection. All reflections from sets of planes in the same $\{hkl\}$ family which have the same angle ω relative to the surface normal will contribute. For example, looking at Fig. 1(a) we can see that in GIXS geometry ($\omega=90°$), a bcc $\{222\}$ reflection will have contributions from $(\bar{2}22)$, $(2\bar{2}2)$, $(2\bar{2}\bar{2})$, and $(\bar{2}2\bar{2})$. Each of these sets of planes might have a different orientation relative to the stress tensor with the result that all crystallographically equivalent directions are not necessarily subjected to the same stress state. Therefore, reflections from the films yield an average of d spacings from several different strain states. The expected d spacing of a given reflection when a stress tensor, σ, is applied, will be the average over all equivalent crystallographic directions, i.e., all reflections in the same family at the same angle, ω. Inspection of Fig. 1 shows that this can be accomplished by averaging for the bcc phase,

$$d_{\text{av}}(hkl)=[d(hkl)+d(hk\bar{l})]/2\ , \tag{6}$$

and for the fcc phase,

$$d_{\text{av}}(hkl)=[d(hkl)+d(lhk)+d(klh)]/3\ . \tag{7}$$

We define the reference frames for the two constituents, shown in Fig. 2. As shown in Fig. 2(a), the bcc Mo

has [110] as the surface normal and [001] and [1$\bar{1}$0] are two perpendicular directions in the sample plane. These three vectors form an orthogonal basis. A similar basis can be defined for fcc Ni with [111] texture, with [1$\bar{1}$0] and [11$\bar{2}$]as the in-plane directions [Fig. 2(b)].

An arbitrary stress state in the film reference frame can be represented as a tensor:

$$\sigma_{ij}=\begin{bmatrix}\sigma_{11} & \sigma_{12} & \sigma_{13}\\ \sigma_{12} & \sigma_{22} & \sigma_{23}\\ \sigma_{13} & \sigma_{23} & \sigma_{33}\end{bmatrix} .$$

For a thin film on a substrate, the out-of-plane components, σ_{11}, σ_{12}, and σ_{13}, vanish. Furthermore, we lose no generality if we represent the in-plane components by their principal values, which we call σ_2 and σ_3. This requires that we be able to apply this stress in an arbitrary in-plane direction, corresponding to a rotation about the surface normal. We accomplish this by applying the stress in reference frames rotated by an arbitrary in-plane angle. These reference frames are illustrated in Fig. 2, where the primed reference frames for each constituent are rotated by an arbitrary in-plane angle relative to the

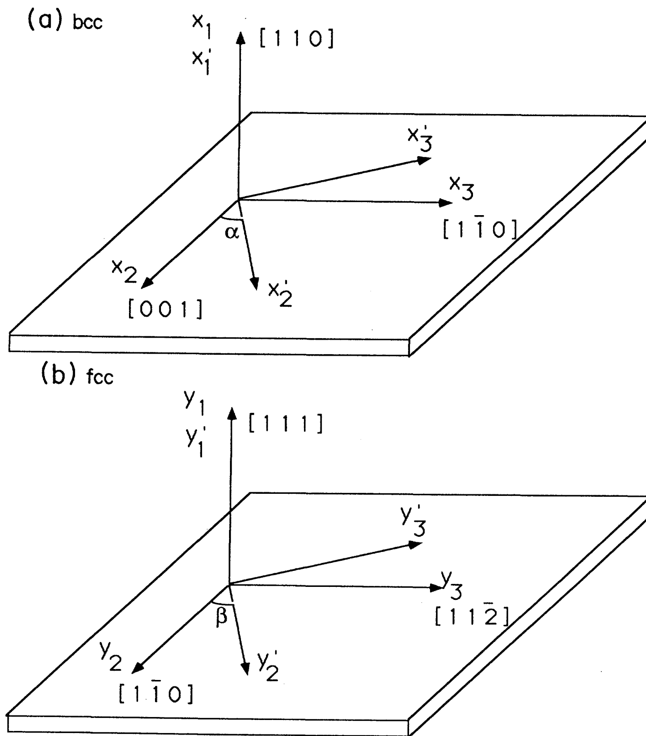

FIG. 2. Orthogonal reference frames for bcc and fcc constituents. (a) bcc constituent, showing the surface normal parallel to the [110] direction and the in-plane directions [001] and [1$\bar{1}$0]. The primed frame is rotated by an in-plane angle α. (b) fcc constituent, showing the surface normal parallel to the [111] direction and the in-plane directions [1$\bar{1}$0] and [11$\bar{2}$]. The primed frame is rotated by an in-plane angle β.

original unprimed reference frames. For bcc Mo, the angle α is the amount by which the principal stress axes are rotated in the plane of the film relative to the [001] and [1$\bar{1}$0] directions. For fcc Ni, the angle β is the amount by which the principal stress axes are rotated in the plane of the film relative to the [1$\bar{1}$0] and [11$\bar{2}$] directions.

Treating each constituent separately, we apply the stress state,

$$\sigma_i=\begin{bmatrix}0 & 0 & 0\\ 0 & \sigma_2 & 0\\ 0 & 0 & \sigma_3\end{bmatrix} ,$$

in the primed reference frame. Note that substrate-interaction stresses produce an equal-biaxial stress state, i.e., $\sigma_2=\sigma_3$, so that the in-plane stress is independent of α,β. By allowing the stress state to have unequal principal components at an arbitrary in-plane angle, we have included the possibility of coherency stresses between dissimilar crystal structures.

Using bulk elastic constants, C_{11}, C_{12}, and C_{44}, we then calculate the strain associated with the stress for each constituent. We calculate lattice spacings for any set of atomic planes as a function of σ_2, σ_3, d_0, and α or β. We fit our calculation to the observed plane spacings, using these four quantities as fitting parameters.

We find that, while the stresses we calculate depend on α or β, the fitting quality is independent of these angles due to the averaging introduced by Eqs. (6) and (7). However, for any α or β, we find unequal values for the principal stresses σ_2 and σ_3, leading to the conclusion that there are coherency stresses between fcc Ni and bcc Mo. As pointed out in Sec. II, the orientation of the principal stress axes is related to the epitaxial orientation between the constituents. If we could determine the orientation of the principal axes of the stress (in this case the angles α or β), we could deduce the epitaxial orientation. However, since the fitting is not sensitive to these angles, this method cannot be used to deduce epitaxial orientations in polycrystalline films.

Conversely, if we assume a reasonable epitaxial orientation, we can deduce an orientation for the principal stresses. For the present case of Ni/Mo, geometric arguments[20] and interface energy calculations[21] suggest that the Nishiyama-Wasserman orientation is the most reasonable. In this orientation, the in-plane directions $[001]_{\rm bcc}$ and $[1\bar{1}0]_{\rm fcc}$ are parallel, with a 26% mismatch in plane spacing, and the in-plane directions $[1\bar{1}0]_{\rm bcc}$ and $[11\bar{2}]_{\rm fcc}$ are parallel with a 3% mismatch in plane spacing. Hence, we expect the principal stresses to lie along these directions, and with this assumption we can find values for σ_2 and σ_3 from our fit to observed lattice-plane spacings. We choose σ_2 to be along the $[001]_{\rm bcc}$ and $[1\bar{1}0]_{\rm fcc}$ directions, and σ_3 to be along the $[1\bar{1}0]_{\rm bcc}$ and $[11\bar{2}]_{\rm fcc}$ directions, i.e. $\alpha=\beta=0$ (Fig. 2).

Figure 3 shows the measured Mo lattice parameter, obtained from in-plane GIXS measurements, as a function of in-plane orientation (the angle ϕ is measured counter clockwise from the [001] direction). Also shown (solid line) is the result of our calculation, using fitted values for

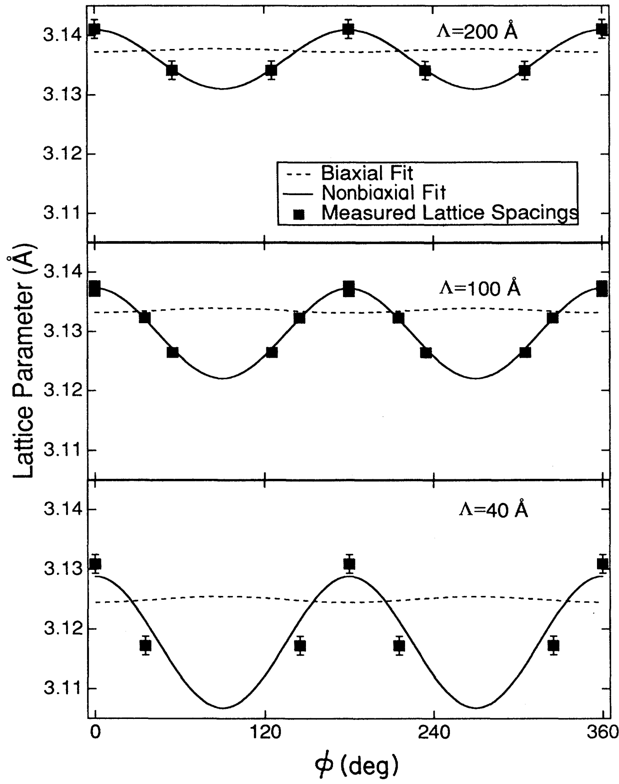

FIG. 3. In-plane Mo lattice parameter vs in-plane direction for three bilayer periods. The angle ϕ is measured from the [001] direction. Values obtained from GIXS measurements are shown as squares, the solid line is calculated from fitted values of σ_2, σ_3, and d_0. The dashed line is calculated in the same manner with the constraint that $\sigma_2=\sigma_3$.

σ_2, σ_3, and d_0. For each bilayer the agreement is greatly improved over that obtained assuming an equal-biaxial stress state, $\sigma_2=\sigma_3$ (dashed line). The data is best fitted when $\sigma_2\neq\sigma_3$, which indicates the presence of coherency stresses between the structurally dissimilar constituents. It should be noted that this behavior persists regardless of what epitaxial arrangement is chosen; it is not a consequence of the assumption of the Nishiyama-Wasserman orientation. The assumption simply allows the calculation of the magnitudes of each stress component.

The nature of coherency stresses is such that they are equal and opposite in the two constituents. Therefore we can write total principal components of the stress for each component, $\sigma_{2,3}^{\mathrm{Mo}}$ and $\sigma_{2,3}^{\mathrm{Ni}}$, as

$$\begin{aligned}\sigma_2^{\mathrm{Mo}}&=\langle\sigma\rangle-\sigma_2^E\,,\\ \sigma_3^{\mathrm{Mo}}&=\langle\sigma\rangle-\sigma_3^E\,,\\ \sigma_2^{\mathrm{Ni}}&=\langle\sigma\rangle+\sigma_2^E\,,\\ \sigma_3^{\mathrm{Ni}}&=\langle\sigma\rangle+\sigma_3^E\,,\end{aligned} \tag{8}$$

where $\sigma_{2,3}^E$ are the magnitudes of the principal coherency stresses, and $\langle\sigma\rangle$ is the global equal-biaxial substrate interaction stress (see the reference frames above for the definitions of directions 2 and 3). Assuming that the coherency stresses are equal and opposite in the two constituents, and that the substrate-interaction stress acts equally on both constituents of the multilayer, allows us to calculate the coherency stresses which arise from the epitaxial arrangement.

Figure 4 shows the coherency and substrate-interaction stresses as a function of $1/\Lambda$, where Λ is the bilayer

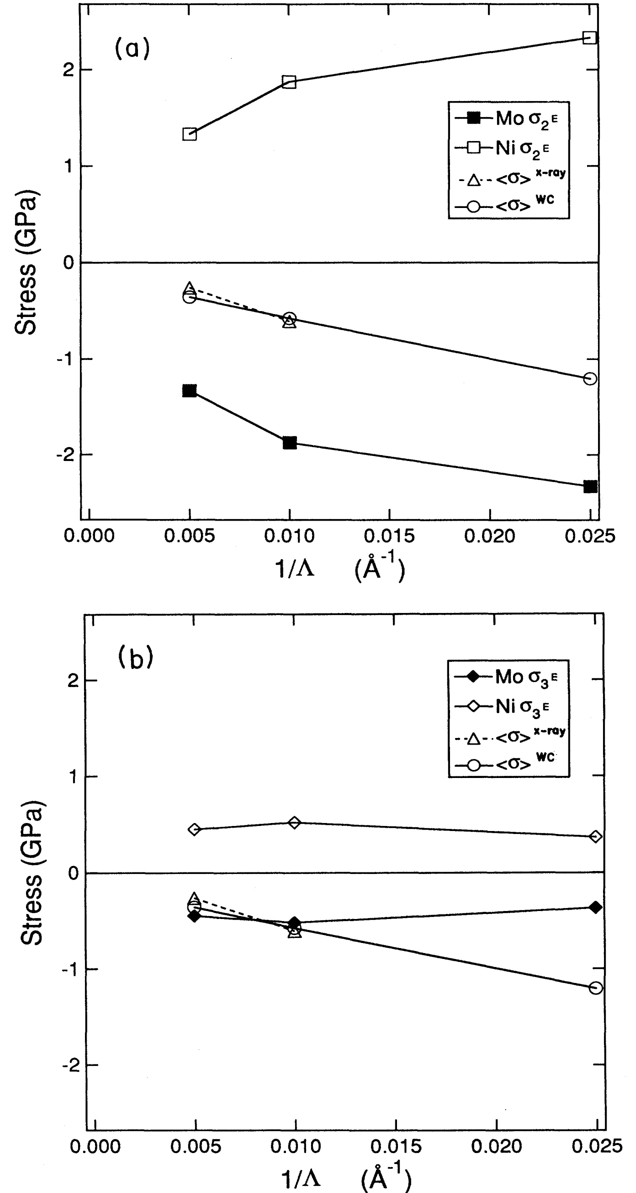

FIG. 4. Components of the stress in the plane of the film vs inverse bilayer period. (a) Mo σ_2^E is the coherency stress in direction 2, [001], of the Mo. Ni σ_2^E is the coherency stress in direction 2, [110], of the Ni. (b) Mo σ_3^E is the coherency stress in direction 3, $[1\bar{1}0]$, of the Mo. Ni σ_3^E is the coherency stress in direction 3, $[11\bar{2}]$, of the Ni. The substrate-interaction stress as measured by x-ray and wafer-curvature methods are given by $\langle\sigma\rangle^{\text{x-ray}}$ and $\langle\sigma\rangle^{\mathrm{WC}}$, respectively.

period. Note that the magnitudes of both these stresses increase with decreasing bilayer period. As pointed out earlier, the increase in magnitude of the coherency stresses is expected due to the balance between elastic and interface defect energies. The increase in substrate-interaction stress with decreasing bilayer period has been observed in Au/Ni.[11] While this substrate-interaction stress may be due to any of the sources mentioned in Sec. II, its variation with bilayer period is explained by the thickness-dependent yield-stress model. We should also point out that, while the values we find for the coherency stresses from x-ray measurements are dependent on our choice of principal axis direction, the substrate stress calculated from the x-ray measurements was not, and thus was not dependent on the choice of the epitaxial orientation. In addition, the trend of increasing coherency stresses with decreasing bilayer period was also independent of the choice of epitaxial orientation.

Also plotted in Fig. 4 are the values for $\langle \sigma \rangle$ obtained from wafer-curvature measurements. The excellent agreement between $\langle \sigma \rangle$ determined from wafer-curvature and lattice-parameter measurements implies that, for this system, interface-contraction stresses are not significant. As discussed in Sec. II, interface-contraction stresses will cause a lack of balance between the constituent and substrate stresses. The substrate stress we calculate from the change in the lattice parameter of the constituents is the same as that we observe to be bending the substrate. Therefore stresses due to interface contraction are not playing a significant role.

B. Nonelastic effects

Once we have determined the strain state and d_0 for each constituent, we can calculate the growth-direction lattice parameters, $d_\perp^{a,b}$. We can then take their weighted average as in Eq. (2) and find $\bar{d}_\perp^B$. In the present case, we have equal layer thicknesses, so we have

$$d^{\mathrm{Mo}}N^{\mathrm{Mo}}=d^{\mathrm{Ni}}N^{\mathrm{Ni}} . \tag{9}$$

This yields, for $\bar{d}_\perp^B$,

$$\bar{d}_\perp^B=\frac{d_\perp^{\mathrm{Mo}}d_\perp^{\mathrm{Ni}}}{d_\perp^{\mathrm{Mo}}+d_\perp^{\mathrm{Ni}}} . \tag{10}$$

This average growth-direction d spacing, found from GIXS and asymmetric measurements, represents the effects of elastic strains on the bulk lattice parameters of the constituents. We can compare this value to $\bar{d}_\perp^S$ obtained from the central superlattice satellite in symmetric diffraction [Eq. (1), Sec. III A], which also includes the effect of anomalous interface spacings due to the interface morphology or relaxation effects.

Figure 5 compares $\bar{d}_\perp^B$ found from GIXS and asymmetric measurements with $\bar{d}_\perp^S$ obtained from symmetric diffraction. Both show an increase as the bilayer period decreases. In all cases except the $\Lambda=200$ Å sample the agreement between the two is excellent. (The disagreement at $\Lambda=200$ Å may be due to the difficulty associated with identifying the position of the central superlattice satellite which is very weak in this case.) This agreement

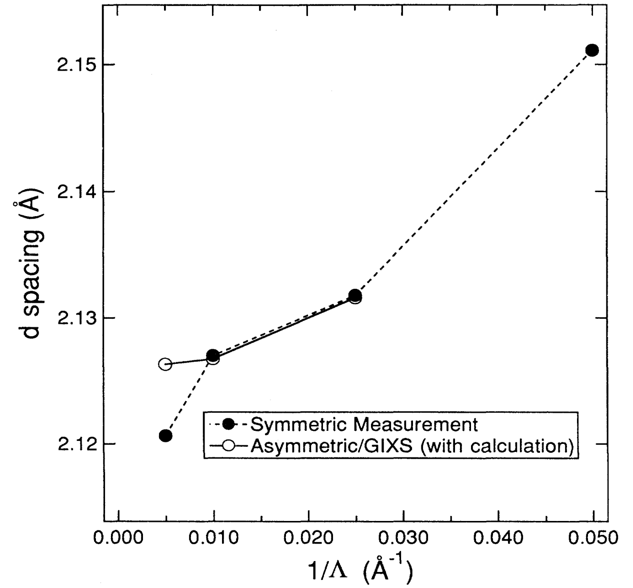

FIG. 5. Average d spacing in the growth direction vs the inverse of the layering period. The solid line and/or open circles was (were) calculated from lattice-parameter measurements in other directions as described in the text. The dashed line and/or solid circles was (were) actually measured with the scattering vector normal to the samples.

reveals that the expansion in the growth direction is due to Poisson effects associated with increasing coherency and substrate-interaction stresses. This is contrary to an earlier suggestion that this expansion was due to an interface d spacing that is larger than that of the constituents.[2]

Figure 6 shows the unstrained lattice parameter as a function of the reciprocal of the bilayer period. The Mo lattice parameter decreases by $\sim 0.2\%$ and the Ni lattice parameter increases by $\sim 0.4\%$. This will produce a net average expansion of $\sim 0.1\%$ of the entire multilayer structure. Thus this bulk expansion of the unstrained lattice parameters does not play a significant role in the observed $\sim 1\%$ out-of-plane expansion in the growth direction shown in Fig. 5. It is possible that the changes in unstrained lattice parameters are due to electron-transfer effects,[4] but a more likely explanation is alloying, which increases as the bilayer period decreases. The alloying content can be estimated using the method of King,[22] and in the most extreme case (40-Å-bilayer-period sample), these correspond to a 93% Mo phase and a 93% Ni phase.

C. Particle size and inhomogeneous strains

The width of GIXS peaks increased with decreasing bilayer period. This can result from decreasing particle size or increasing inhomogeneous strain. These two effects have behaviors which differ as a function of the scattering vector, q. ($q=4\pi\sin\theta/\lambda$, where θ is the Bragg angle and λ is the x-ray wavelength.) A polycrys-

talline sample with average particle size, L, will produce peak widths, $(\Delta q)_{PS} \approx 2\pi/L$, while inhomogeneous strain with a rms value $\langle \epsilon^2 \rangle^{1/2}$ will have $(\Delta q)_{IS} \approx \langle \epsilon^2 \rangle^{1/2} q$. Assuming that the peak widths can be added, the intercept of a plot of Δq versus q for each sample will yield L, while the slope will be $\langle \epsilon^2 \rangle^{1/2}$.[23] Performing this analysis on GIXS peaks gives us the in-plane particle size $L_{\parallel}$ and in-plane strain variance $\langle \epsilon^2 \rangle_{\parallel}^{1/2}$.

Figure 7 shows $L_{\parallel}$ as a function of bilayer period, showing that the particle size is about 100 Å, independent of bilayer period. This indicates that the wider peaks at lower periods were not due to changes in the crystal size. On the other hand, Fig. 8 shows that $\langle \epsilon^2 \rangle_{\parallel}^{1/2}$ increases as the bilayer period decreases. As shown in Fig. 9, this increase in $\langle \epsilon^2 \rangle_{\parallel}^{1/2}$ scales with the average equal-biaxial stress, $\langle \sigma \rangle$. We postulate that as the average equal-biaxial stress increases, the variance increases, yielding a proportionally larger rms stress and strain.

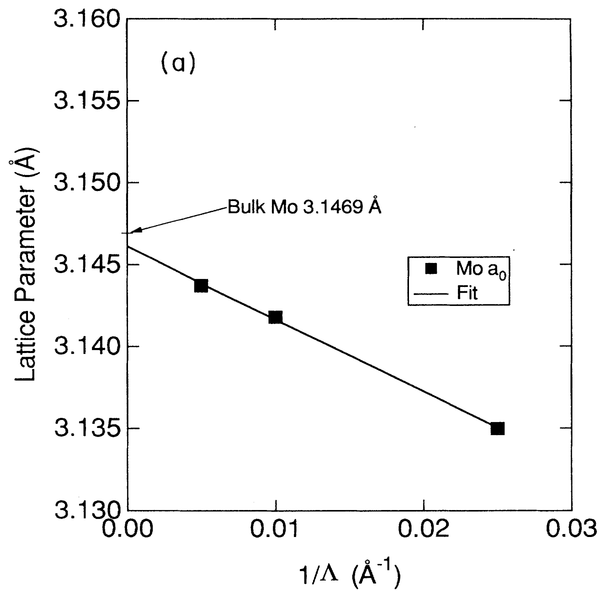

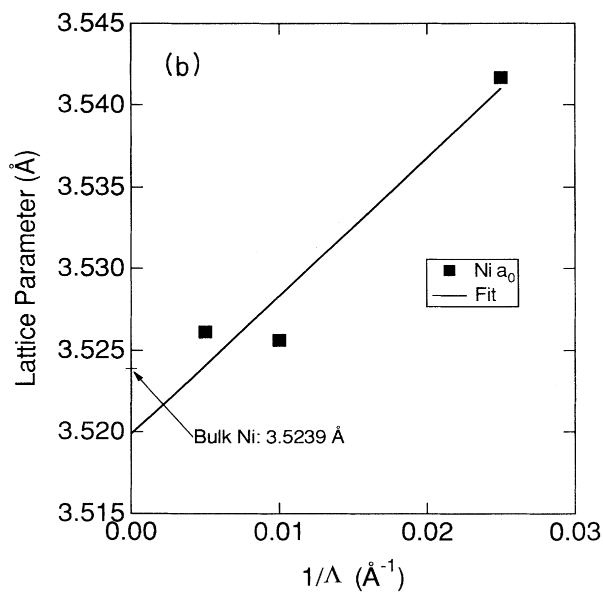

FIG. 6. Unstrained lattice parameter of (a) Mo and (b) Ni vs inverse bilayer period. The solid lines are fits to the data.

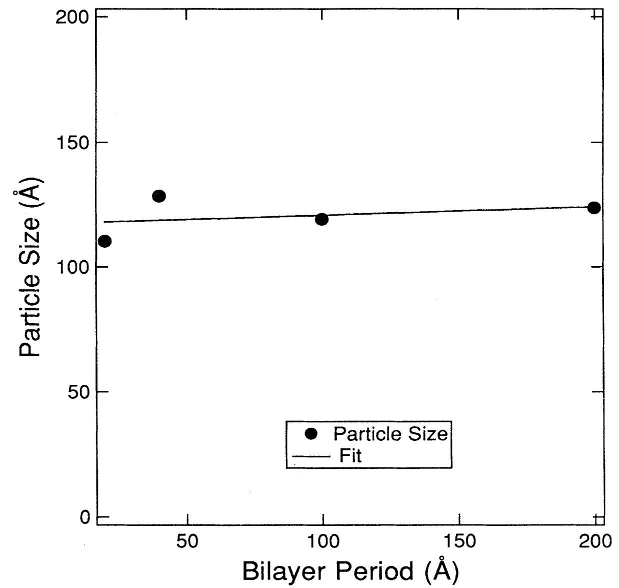

FIG. 7. In-plane particle size vs layering period. The solid line is a fit to the data.

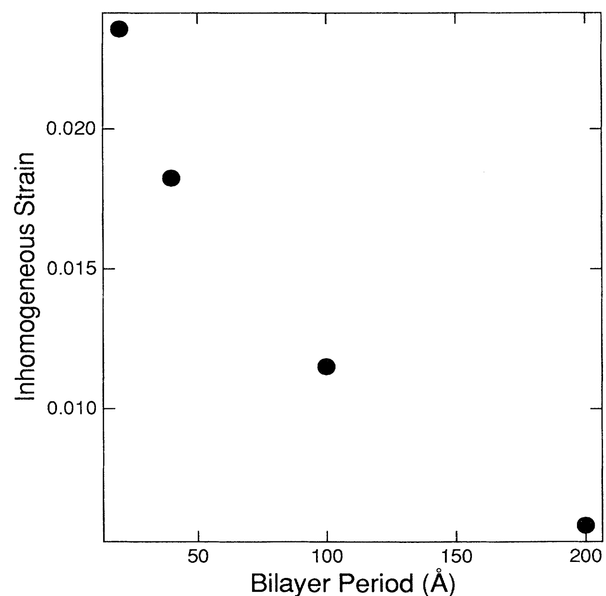

FIG. 8. Inhomogeneous strain, $\langle \epsilon^2 \rangle^{1/2}$, vs bilayer period.

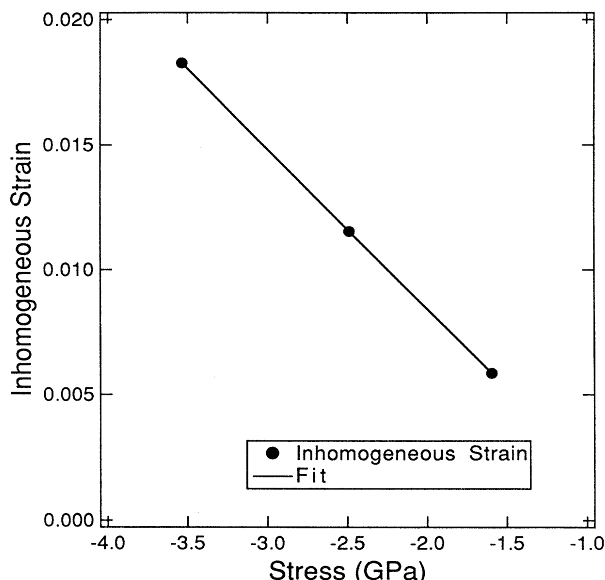

FIG. 9. Inhomogeneous strain, $\langle \epsilon^2 \rangle^{1/2}$, vs substrate-interaction stress, $\langle \sigma \rangle$.

V. CONCLUSIONS

We conclude that the stress state in Mo/Ni multilayers is dominated by substrate-interaction stresses and coherency stresses. These increase as the bilayer period decreases, and the previously observed expansion in the out-of-plane lattice spacing is due to the Poisson expansion associated with the in-plane compression from these stresses. The coherency stresses are not equal-biaxial, reflecting the symmetry mismatch between the mating planes. If we assume the Nishiyama-Wasserman orientation, we see that the largest stress occurs in the direction of the largest mismatch. We find no evidence for interface-contraction stresses or interface-dilation strains. The small changes in the unstrained lattice parameters can be attributed to alloying.

ACKNOWLEDGMENTS

One of us (J.A.B.) would like to acknowledge partial support by the U.S. National Science Foundation (NSF). Support for another of us (S.B.) was provided by the U.S. Department of Energy (DOE), Office of Basic Energy Sciences. Part of this work was done at the Stanford Synchrotron Radiation Laboratory, which is supported by the DOE, Division of Chemical Sciences, and part of this work was performed at the Stanford Center for Materials Research under the NSF Materials Research Laboratory program. Thanks are extended to Professor W.D. Nix, Professor Frans Spaepen, and Professor Robert Cammarata for helpful discussions, and to Fred von Pressig for making the wafer-curvature measurements.

[1]M.R. Khan, C.S.L. Chun, G.P. Felcher, M. Grimsditch, A. Kueny, C.M. Falco, and I.K. Schuller, Phys. Rev. B **27**, 7186 (1983).
[2]B.M. Clemens and G.L. Eesley, Phys. Rev. Lett. **61**, 2356 (1988).
[3]W.R. Bennett, J.A. Leavitt, and C.M. Falco, Phys. Rev. B **35**, 4199 (1987).
[4]I.K. Schuller and A. Rahman, Phys. Rev. Lett. **50**, 1377 (1983).
[5]J.W. Matthews, in *Epitaxial Growth* , edited by J.W. Matthews (Academic, New York, 1975), p. 559.
[6]W.D. Nix, Metall. Trans. A **20**, 2217 (1989).
[7]D.W. Hoffman and J.A. Thornton, Thin Solid Films **45**, 387 (1977).
[8]C.W. Mays, J.S. Vermaak, and D. Kuhlmann-Wilsdorf, Surf. Sci., **12**, 134 (1968).
[9]R.C. Cammarata and K. Sieradzki, Appl. Phys. Lett. **55**, 1197 (1989).
[10]K. Sieradzki (private communication).
[11]S.P. Baker and W.D. Nix, in *Thin Films: Stresses and Mechanical Properties* II, edited by W. C. Oliver, M. Doerner, G. M. Pharr, and F. R. Brotzen, Mater. Res. Soc. Symp. Proc. No. 188 (Materials Research Society, Pittsburgh, 1990).
[12]R.C. Cammarata and K. Sieradzki, Phys. Rev. Lett. **62**, 2005 (1989).
[13]J.A. Ruud, A. Witvroum, and F. Spaepen, *in Defects in Materials,* edited by P. D. Bristowe, J. E. Epperson, J. E. Griffith, and Z. Liliental-Weber, Mater. Res. Soc. Symp. Proc. No. 209 (Materials Research Society, Pittsburgh, 1991).
[14]D. Wolf and J.F. Lutsko, Phys. Rev. Lett. **60**, 1170 (1988).
[15]B.M. Clemens, J. Less-Common Met. **140**, 57 (1988).
[16]W.P. Lowe and T.H. Geballe, Phys. Rev. B **29**, 4961 (1984).
[17]P.A. Flinn and G.A. Waychunas, J. Vac. Sci. Technol. **B 6**, 1749 (1988).
[18]P.H. Fuoss and S. Brennan, Annu. Rev. Mater. Sci **20**, 365 (1990).
[19]P.A. Flinn, D.S. Gardner, and W.D. Nix, IEEE Trans. Electron Devices, **ED-34**, 689 (1987).
[20]H. Homma, K- Y. Yang, and I.K. Schuller, Phys. Rev. B **36**, 9435 (1987).
[21]E. Bauer and Jan. H. van der Merwe, Phys. Rev. B **33**, 3657 (1986).
[22]H.W. King. J. Mater. Sci. **1**, 84 (1966).
[23]L.H. Schwartz and J.B. Cohen, *Diffraction From Materials* (Springer-Verlag, New York, 1987).